A New Multi-grid 3-D TLM Algorithm for Simulation of Microwave FSS

M. I. Sobhy, *BSc PhD CEng FIEE MIEEE*, M. H. Abd El-Azeem, *BSc*, and K. W. Royer, *BSc MIEE*, Electronic Engineering Laboratories, University of Kent at Canterbury, Canterbury, Kent, CT2 7NT.

Abstract — This paper describes and demonstrates a new TLM multi-grid algorithm which allows arbitrary mesh dimension changes. Its use is demonstrated in the modelling of Frequency Selective Surfaces (FSS) used in microwave antenna systems where the mesh can be adjusted to describe arbitrary dimensions precisely. The algorithm demonstrates good numerical stability and has been applied to numerous Symmetric Condensed Node (SCN) TLM problems.

I. Smooth Variable Mesh

Multi-grid algorithms are used in TLM modelling to reduce simulation time and memory requirements [4], [5]. This multi-grid algorithm provides a means to interface SCN meshes whose ratios are arbitrary. Fig. 1 shows two such meshes (drawn in 2-D for clarity) and the interface between them. At the interface between meshes the SCN arm potentials in mesh A do not connect with those in mesh B. They differ spatially and temporally because spatial variation Δl is proportional to the nodal time step Δt [8]. Fig. 2 shows the relationship between the end of the SCN arms on the interface plane of mesh A and B, bounded by a TEM line consisting of two electric and two magnetic walls. The two potentials on the ends of each SCN are mirrored by the Magnetic and Electric walls to yield information about the potentials beyond the bounding walls. This information is vital to the interfacing of the potentials between meshes.

In practice the problem can be decoupled into a temporal correction followed by a spatial correction. If the ends of the nodes between meshes A and B are spatially the same, then problem is reduced to a temporal problem because Δt differs on the two interfaces. The scattering algorithms for the meshes are identical, excepting the connection algorithms that differ on the interface. Following a sequence of scattering events, one unconnected mesh face will always be retarded in time with respect to (w.r.t.) the surrounding meshes, so information regarding future incoming impulses is available. Such information allows the incoming impulses, for the retarded mesh interface, to be estimated from the potentials arriving from the surrounding interfaces. In this algorithm, it is assumed that impulses arriving from neighboring meshes have a constant DC potential over Δt. This allow integrations to be made over fractions of a time step (the output from a TLM node is considered to be impulsive). The potential injected into the retarded mesh is calculated by integrating w.r.t. the time the potential from the previous iteration to the present divided by the time interval Δt, in order to insures that,

$$\int_0^T \frac{E_A}{\Delta l_A}\delta t \;=\; \int_0^T \frac{E_B}{\Delta l_B}\delta t. \qquad (1)$$

E_A = SCN potential at any pt. P in mesh A on interface,
E_B = SCN potential at any pt. P in mesh B on interface,
$\Delta l_A \& \Delta l_B$ = SCN sizes in meshes A & B.

Despite this, energy is not conserved [5] because energy passing the boundary is a function of E^2 and the *r.m.s.* values of E_A and E_B differ. In this technique the standard TLM scattering and connection procedures [8] are altered in such a way that dimensionally different meshes scatter and connect at differing rates.

Following the temporal correction between meshes A and B their spatial positions are re-mapped. By employing boundary symmetries a mesh of potentials greater than that dictated by the connecting cuboid face is produced. This face has two sets of SCN arm potentials (ie a z-plane has E_x and E_y potentials) and each set is treated separately. A 2-D natural bi-cubic spline is fitted through each set of points. These splines are then used to evaluate two sets of points spatially

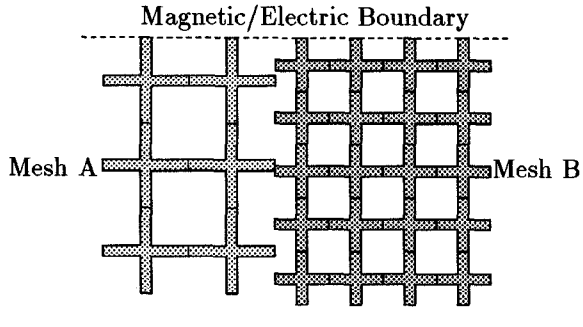

Fig. 1. An Example of Multi-grid in TLM.

0-7803-3246-6/96/$5.00 © IEEE

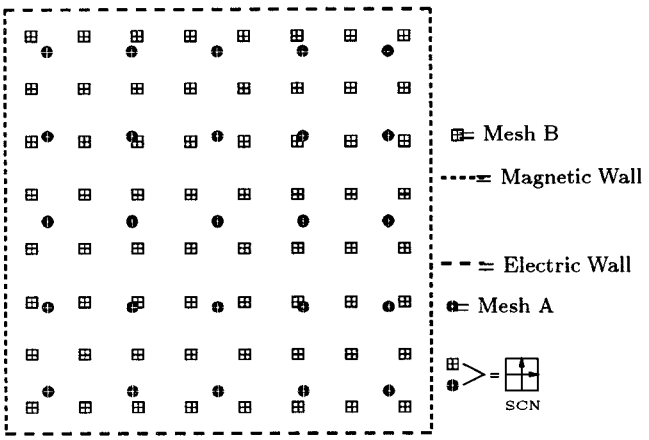

Fig. 2. Interface between meshes in Fig. 1.

re-mapped for the opposing cuboid. These re-mapped potentials are injected into the opposing SCN arms to complete the connection algorithm. Initially, this procedure seems numerically intensive. However, it is only employed on graded-mesh interfaces and hence only adds a few percent to the total simulation time. In other problems additional boundary symmetries must be applied for a few nodes beyond the edges of the cuboid face in order to complete the spline.

Considerations are necessary to ensure the algorithm's stability. Other multi-grid algorithms have shown instability because energy is not conserved. Careful choice of excitations is important because impulse functions result in instabilities due to the very high frequency components contained in such excitations. This is partly due to spurious modes in the SCN mesh [6], [7]. In resonant systems, problems arise because impulses pass across boundaries several times and, as a result, increase the system energy at selected frequencies. For a wide range of TLM problems studied by our research group, this multi-grid algorithm improves simulation time and accuracy.

The accuracy of the algorithm is tested using the micro-strip line shown in fig. 3 employing multi-grid. The SCN mesh is changed by a ratio of two without changing the structure dimensions. The magnitude of the reflection of a Gaussian pulse propagating along the line is measured at the discontinuity. As a measure of confidence, the impedance of the stripline was calculated separately by TLM simulation in a 1mm mesh and then in a 0.5mm mesh, these results differ because the fields are modeled more accurately in the finer mesh. Using these simulated impedances S_{11} was calculated using,

$$S_{11} = \frac{Z_f - Z_c}{Z_f + Z_c}. \qquad (2)$$

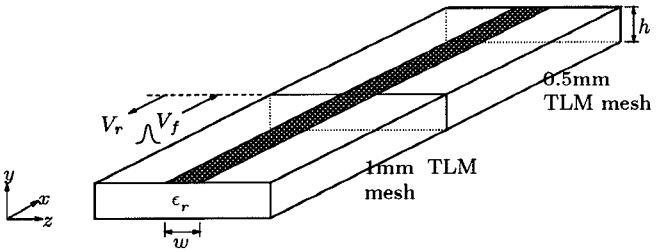

Fig. 3. Test Stripline for Multi-grid Testing, w = 2mm, h = 2mm, ϵ_r = 2.2.

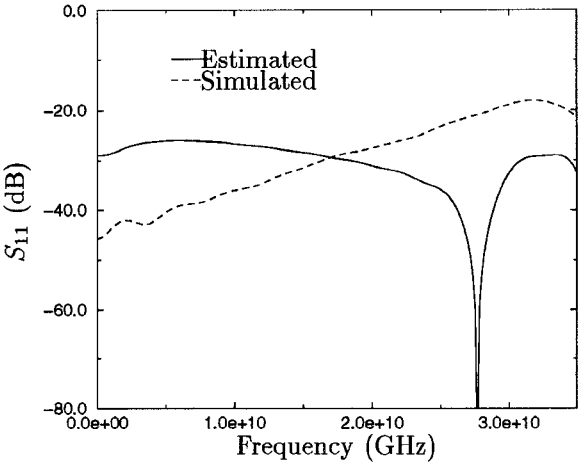

Fig. 4. Results from Multi-grid reflection measurements.

Where Z_f and Z_c are the simulated impedances in the 0.5mm and 1mm meshes respectively. Following this the simulation was run and the reflection from the discontinuity measured. Fig. 4 shows the estimated (eqn. 2) and simulated reflection from the mesh change. The multi-grid algorithm gives a better result at low frequencies than expected. The dip in the calculated response is due to the measured impedances being identical as this frequency, their is a limit to the accuracy of the impedance measurement resulting from the choice of the field integration path around the conductor. From this graph it can be seen that their is a limit to multi-grid algorithms, this limit is not a function of the numerical technique used here but in the accuracy of TLM model in the course mesh.

II. FSS Modelling

TLM modelling of FSS structures demonstrates effectively the use of this multi-grid algorithm. A typical FSS is shown in fig. 5. It consists of a metalisation pattern on a thin flexible low loss substrate. In our initial analysis we will ignore the substrate effects. The problem shown in fig. 5 reduces to the problem shown in fig. 6 by applying electric and magnetic planes of symmetry to the structure.

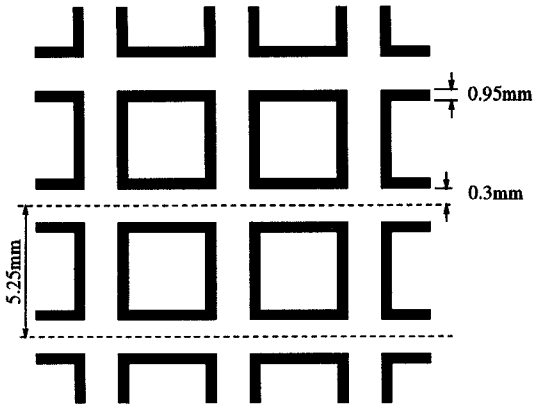

Fig. 5. Section of a typical FSS.

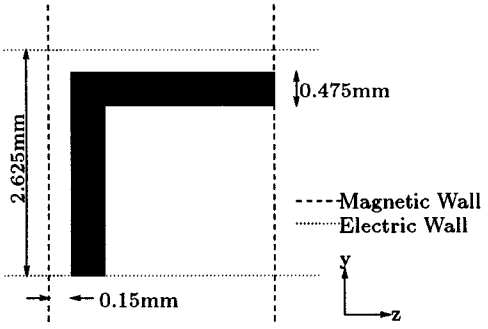

Fig. 6. Reduced FSS model from Fig. 5 following application of planes of symmetry.

The resulting structure of fig. 6 is easily simulated because it is bounded by the TEM line with the FSS tangential to the plates. The structure is excited away from the FSS by a planar TEM E_y Gaussian pulse and measured behind the structure to yield the transmission response. The remaining faces are bounded by setting the reflection coefficient, *rho*, to zero. This technique is applicable because the field is predominately TEM. The distance infront and behind the FSS in fig. 6 should be large compared to the FSS y and z dimensions to ensure the E_y TEM excitation is undisturbed by the FSS and the E_y measurement plane contains predominately a TEM wave.

In practice the metalisations are created by short circuiting the SCN arms, which creates a metalisation patch between the nodes. To simulate the structure in fig. 6 a node size of 0.025mm was chosen to resolve the structure details accurately, the length l, infront and behind the FSS, was chosen to be 26.5mm (10× the y and z dimensions). Without multi-grid this would result in a requirement of 23,373,000 SCN's. By using a course mesh away from the FSS of 0.525mm the memory requirement is reduced to 115,500 nodes. This gives a 202 times reduction in memory requirements, and a larger

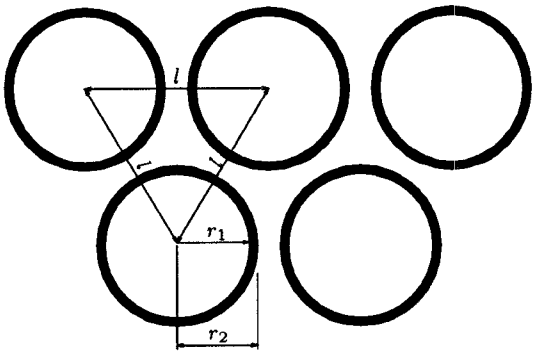

Fig. 7. Simple Circular FSS on dielectric substrate, l = 4.9mm, r_1 = 1.8mm, r_2 = 2.2mm.

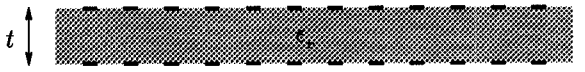

Fig. 8. Cross section of FSS shown in 7, $t = 0.075mm$, $\epsilon_r = 2.33$.

reduction in terms of simulation time [9].

III. Results

Figures 7 and 8 show a simple single layer circular FSS on an equilateral triangular grid [2]. This structure, via symmetry, reduces to the structure shown in fig. 9, the results from the TLM simulation is shown if fig. 10. Two meshes were used to resolve the structure, a 0.0375mm mesh around the metalisations and a 0.1875mm mesh away from the FSS. This results in a total of 104,650 nodes, which using a single mesh would have resulted in 72 times the number of nodes.

Figures 11 and 12 show a complex double layer FSS used for diplexing [3]. These FSS surfaces show a sharp transmission peak generated very close to the edge of the main reflection band, obtained by careful selection of the spacing between the FSS surfaces. The simulated results shown in fig. 13 show a close match to the results measured at a 5° angle of incidence [3].

The slight mismatch is partly due to the simulation being at normal incidence (not at 5°). Also, the dispersion in the TLM mesh makes the higher frequency

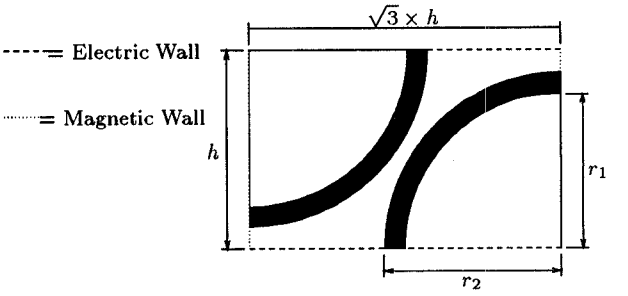

Fig. 9. Simulated model reduced via symmetry, $h = 2.45mm$, $r_1 = 1.8mm$, $r_2 = 2.2mm$.

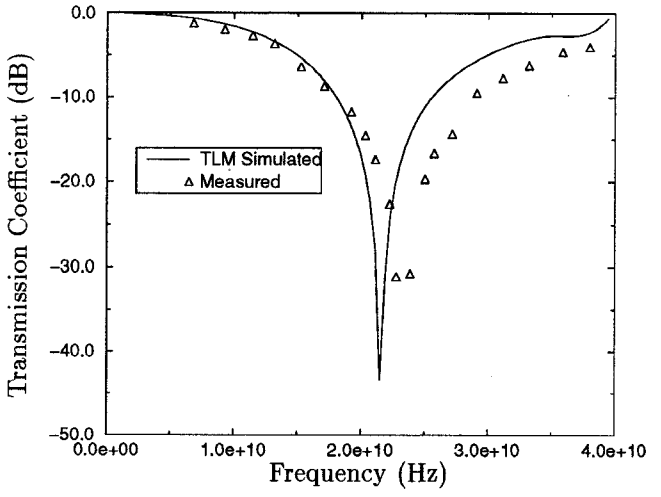

Fig. 10. Results of TLM simulation of structure in Fig. 9.

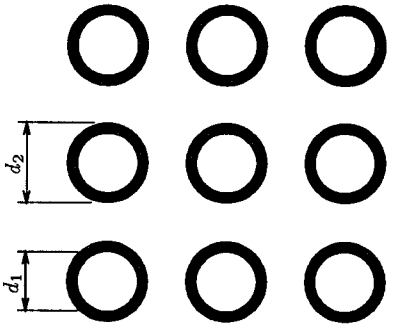

Fig. 11. Circular patterns used in FSS diplexer, $d_1 = 3.61$mm, $d_2 = 4.51$mm.

measurements less accurate. The cut-off frequency of the coarsest mesh was 30GHz which limits the accuracy at the higher frequencies. This problem was modeled using a total of eleven mesh changes to ensure the substrate thickness was resolved accurately and the FSS metalisations were accurately described. In practice 5 megabytes of computer memory was required which is 500 times less the estimated use without the multi-grid algorithm.

Summary

The use of this multi-grid algorithm allows SCN mesh changes to be made relatively freely compared to other techniques [5]. This technique has been employed successfully to resolve small dimensions in FSS structures without the need to employ complex analytical formulae. Additionally a limit to the use of multi-grid algorithms has been demonstrated, and hence a restriction to regions where any multi-grid algorithm may be employed successfully.

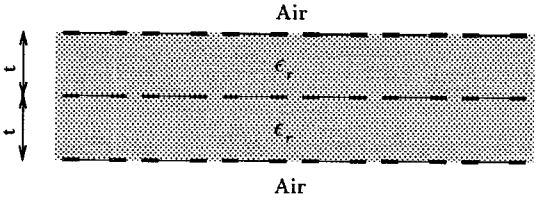

Fig. 12. Cross section of FSS diplexer, $t = 3.1$mm, $\epsilon_r = 2.33$.

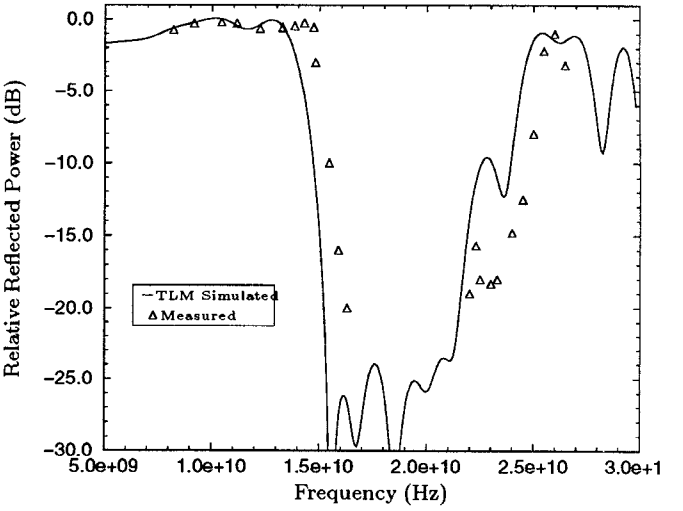

Fig. 13. Results From TLM Simulation shown in Fig. 12.

References

[1] E. A. Parker and R. J. Langley, "Double-Square Frequency Selective Surfaces and their Equivalent Circuit", *Electronic Letters, Vol.19, No.17, pp.675-677.*

[2] E. A. Parker and S. M. A. Hamdy, "Rings as Elements for Frequency Selective Surfaces", *Electronic Letters, Vol.17, No.17, pp.612-614.*

[3] R. Cahill, E. A. Parker and C. Antonopoulos, "Design of Multi-layer Frequency Selective Surface for Diplexing Two Closely Spaced Channels", *Microwave and Optical Technology Letters, Vol.8, No.6, pp.293-296.*

[4] R. H. Voelker and R. J. Lomax, "3-Dimensional Simulation of Integrated-Circuits Using Variable Mesh TLM Method", *Microwave and Optical Technology Letters, 1989, Vol.2, No.4, pp.125-127.*

[5] J. L. Herring and C. Christopoulos, "Multi-grid Transmission Line Modeling Method for Solving Electro-magnetic Field Problems", *Electronics Letters, 1991, Vol.27, No.20, pp.1794-1795.*

[6] Zhizhang Z. Chen, "PhD thesis on TLM modeling", *Chapter 4, Adsorbing And Connecting Boundary Conditions In The TLM Simulations., Department of Electrical and Computer Engineering, University of Victoria, Victoria B. C., Canada.*

[7] J. S. Nielson and W. J. R. Hoeffer, "Generalised Dispersion Analysis and Spurious Modes of 2-D TLM and 3-D TLM Formulations", *IEEE Transactions on Microwave Theory and Techniques, 1993, Vol.41, No.8, pp.1375-1384.*

[8] P. B. Johns, "A Symmetrical Condensed Node for the TLM Method", IEEE Transactions on Microwave Theory and Techniques, 1987, Vol.35, No.4, pp.370-377.

[9] M. I. Sobhy, M. H. Abd El Azeem, K. W. Royer, R. J. Langly, and E. A. Parker "Simulation of Frequency Selective Surfaces (FSS) Using 3D-TLM", *IEE 3rd Int Conference on Computation in Electromagnetics, Bath, UK, April 1996.*